Front. Optoelectron. 2020, 13(1): 12–17
https://doi.org/10.1007/s12200-019-0941-2

RESEARCH ARTICLE

Holographic fabrication of octagon graded photonic super-crystal and potential applications in topological photonics

Oliver SALE[1], Safaa HASSAN[1], Noah HURLEY[1], Khadijah ALNASSER[1], Usha PHILIPOSE[1], Hualiang ZHANG[2], Yuankun LIN (✉)[1,3]

1 Department of Physics, University of North Texas, Denton, TX 76203, USA
2 ECE Department, University of Massachusetts Lowell, Lowell, MA 01854, USA
3 Department of Electrical Engineering, University of North Texas, Denton, TX 76203, USA

Abstract Novel optical properties in graded photonic super-crystals can be further explored if new types of graded photonic super-crystals are fabricated. In this paper, we report holographic fabrication of graded photonic super-crystal with eight graded lattice clusters surrounding the central non-gradient lattices through pixel-by-pixel phase engineering in a spatial light modulator. The prospect of applications of octagon graded photonic super-crystal in topological photonics is discussed through photonic band gap engineering and coupled ring resonators.

Keywords 2D photonic crystal, graded photonic super-crystal, holographic fabrication, photonic band structure

1 Introduction

Diffractive optical element (DOE), such as a phase mask used for the fabrication of fiber Bragg grating, has been a very attractive technique for the holographic fabrication of photonic crystals through one-beam, one DOE and one-exposure method [1,2]. DOE can be used to control the phase profile of a laser beam and generate a desired spatial distribution of the laser intensity. Compared with traditional binary masks, DOE has an advantage of fully using all the incident light power and modulating the light patterns in the beam propagation direction. However, a static DOE cannot be electrically programmed for the control of the laser beam on-the-fly.

A programmable liquid crystal based spatial light modulator (SLM) is a very attractive DOE as it can electronically encode the amplitude or phase of the laser beam in its display of liquid crystal on silicon. The laser beam can be controlled as a tool of dynamic tweezer or micro-rotor [3,4]. The computer-generated hologram displayed in SLM can be used to engineer the phases of interfering for the generation of desired inference patterns with periodic or quasi-periodic, and chiral structures [5–12]. SLMs have been used to fabricate photonic structures with varying lattice orientation, lattice spacing, and filling fraction through innovative synthesis approaches [13–16]. Arbitrary designs of phase patterns were very attractive but they could result in an assignment of several gray levels on a single pixel, consequently leading to a super-lattice effect.

Pixel-by-pixel phase engineering of phase patterns in SLM can produce the highest resolution in the fabricated photonic structure and can also register the desired defects in line with the photonic lattices [17]. Very recently, the pixel-by-pixel phase engineering in checkerboard format in SLM has produced two sets of interfering beams for the fabrication of graded photonic super-crystals (GPSCs) in square lattices where graded lattice clusters formed in square, rectangular, hexagonal and 5-fold symmetries [18–21]. There are three design levels: (a) two gray levels were assigned to the pixels in checkerboard format that produced one set of diffraction spots with a large diffraction angle; (b) two types of checkerboards with different gray levels fill the pixels alternately in clockwise rotation; (c) the checkerboard fills the unit cell of the phase pattern in square or triangular shape that produced the other set of diffraction spots with a small diffraction angle [18–21]. Single reflective optical element (ROE) has been integrated with SLM for large area fabrication of GPSCs with small feature period [20]. The main advantage of using the pixel-by-pixel phase pattern in checkerboard format in SLM was that the same ROE can be used even when different phase patterns for different graded lattice clusters are designed in SLM [20].

Received June 1, 2019; accepted June 28, 2019

E-mail: yuankun.lin@unt.edu

In this paper, octagon GPSCs have been fabricated through 12-beam interference lithography through pixel-by-pixel phase engineering in SLM. The prospect of octagon GPSCs for topological photonics has been discussed in aspects of topological photonic band structures and coupled ring resonators.

2 Design of phase pattern in SLM and experimental conditions

The unit cell of designed phase pattern is shown inside the solid red square in Fig. 1(a). The design of the phase pattern was done by assigning a gray level for each pixel inside the unit cell of 12 × 12 = 144 pixels using the Gimp software. The unit cell is repeated to cover the SLM active area of 1920 × 1080 pixels. The pixel size of the SLM used in this paper is 8 μm × 8 μm. Thus the SLM has an active area of 15.36 mm × 8.64 mm. The unit cell was divided into 8 triangular areas by lines in 0, 45°, 90° and 135° relative to x-axis.

The assignment of gray level was based on the diffraction efficiency of formed phase pattern and simulation of iso-intensity of interference pattern using these efficiencies for the formation of GPSC [18,19]. Gray levels of (184, 254) were used for the assignment of gray levels in checkerboard format for pixels in region (I) inside the unit cell in Fig. 1(a) while (128,254) were used for region (II) inside the unit cell in Fig. 1(a). The checkerboard patterns in regions (I) and (II) were used to alternately fill 8 areas in the whole unit cell in counter clockwise direction. The pixels between two checkerboard formats (along the red lines in Fig. 1(a)) were filled in a way such that a half of pixels were filled with a gray level of 184 and the other half of pixels were filled with 128 as seen along the solid red lines and central dashed purple lines. The gamma curve will apply a phase of 0π into a gray level of 0 and 2π phase into a gray level of 255 when the laser beam was incident onto the phase pattern in the SLM. In general, we can assume the phase is gray level × 2π/255 although the gamma curve is not a perfect linear line in the whole range. We generally avoid using the gray level of 255 because 255 might be explained as 2π or 0π in phase.

Figure 1(b) shows an optical image of diffraction pattern (taken with a cell-phone) when a 532 nm laser is incident onto the phase pattern in the SLM. The camera was tilted to avoid the back-reflection spots. The diffraction spots labeled by 1, 2, 3 and 4 in Fig. 1(b) are due to the diffraction from periodic arrangement of two gray level array such as (184,254) in region (I) in Fig. 1(a) through a Bragg diffraction (2 pixels) × $\sin\theta_1 = m\lambda$, where θ_1 is the diffraction angle as defined in Fig. 2 and m is an integral number. Pair of diffraction spots (6,7), (8,9), (10,11) and (12,6) in Fig. 1(b) are due to the diffraction from periodic arrangement of 24 pixels as indicated by the horizontal or vertical lines in Fig. 1(a) through Bragg equation (24 pixels) × $\sin\theta_2 = \lambda$, where θ_2 is the diffraction angle as defined in Fig. 2. The distance d(2,3) between spots 2 and 3 in Fig. 1(b) is $D(2,3) = 2 \times f_1 \times \tan\theta_1$ and the distance d(8, 9) between spots 8 and 9 is $D(8,9) = 2 \times f_1 \times \tan\theta_2$. The ratio of $d(2,3)/d(8,9)$ is about 12. Because of titled image in Fig. 1(b), the experimental value can be measured by the average of d(2,3) and d(1,4) over the average of d(8,9) and d(5,12), which is 11.9. There are also strong diffractions in diagonal directions in Fig. 1(b) due to periodic array of pixels indicated by the solid red lines in Fig. 1(a). The overlap of diffraction in vertical (horizontal) and diagonal directions, as indicated by the solid blue (blue) and solid red lines in Fig. 1(a), respectively, can help determine the azimuthal angle γ for beam 5 in Fig. 1(b) which can be calculated by $\gamma = \arctan(1/2) = 26.57°$ relative to x-axis. The measured value for the angle in Fig. 1(b) for

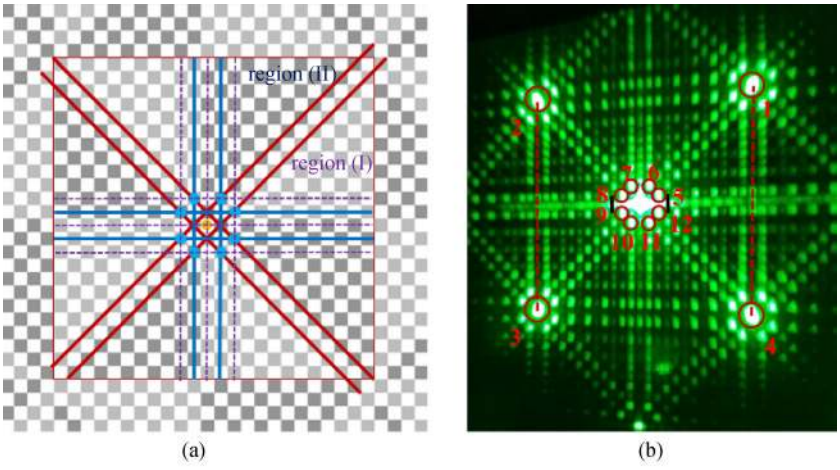

Fig. 1 (a) Designed phase pattern in a unit cell indicated by the solid red square. The pixels were assigned with different gray level pairs in checkerboard format in regions (I) and (II). Lines indicate the periodic unit for the diffraction. (b) Optical image of diffraction pattern of 532 nm laser from the phase pattern in SLM. 12 beams, indicated by red circles, pass through the Fourier filter for multi-beam interference. The cell-phone camera was tilted to avoid the back-reflection spots

beam 5 is 26.6°. The azimuthal angles for beams 6 – 12 are assigned to be 90° – γ, 90° + γ 180°–γ, 180° + γ, 270°–γ, 270° + γ, and 360°–γ, respectively. The size change of the square unit cell in the phase pattern will not change the azimuthal angles of these 12 beams. However, such a change can lead to octagon GPSCs with a different unit super-cell size for device applications.

Figure 2 shows the optical setup for the holographic fabrication of GPSCs. A laser beam with a wavelength of 532 nm (Cobolt Samba 50 mW) was expanded and collimated by using a spatial filter and lens. The laser's polarization is along the longer side of SLM and is incident with an incident angle of 4°. The laser beam was modulated in phase by the phase pattern displayed in the SLM (Holoeye PLUTO). The diffraction spots from the phase pattern are collected through lens1 and filtered by a Fourier filter at the Fourier plane so that only beams 1 – 12 in Fig. 1(b) can pass through. 4*f* imaging system was used with a focal length of $f_1 = 400$ mm and $f_2 = 200$ mm for lens 1 and lens 2, respectively. The 12 beams were overlapped through lens 2 and exposed to a photo sensitive mixtures of dipentaerythritol penta/hexaacrylate (DPHPA) monomer, photo initiator rose bengal, co-initiator *N*-phenyl glycine (NPG), and chain extender *N*-vinyl pyrrolidinone (NVP) [18]. The mixture was spin-coated on a glass slide with a speed of 2500 r/min for 30 s. The GPSC sample was developed in PGMEA for 5 min, rinsed by isopropanol for 1 min and then dried.

3 Multi-beam interference lithography and results

The intensity $I(r)$ of 12 beam interference can be described by Eq. (1):

$$I(r) = \langle \sum_{i=1}^{12} E_i^2(r,t) \rangle + \sum_{i<j}^{12} E_i E_j \hat{e}_i \cdot \hat{e}_j \cos[(k_j - k_i) \cdot r + (\delta_j - \delta_i)], \quad (1)$$

where E, k, δ, $\hat{e}$ are the electric field amplitude, the wave vector, the initial phase, and the electric field polarization direction, respectively.

The wavevectors for beams 1 – 4 can be described as $k(\sin\alpha_1\cos O_{1\text{-}4}, \sin\alpha_1\sin O_{1\text{-}4}, \cos\alpha_1)$, where the angle $O_{1\text{-}4}$ is 45°, 135°, 225°, and 315°, respectively. The wavevectors for beams 5 – 12 can be described by $k(\sin\alpha_2\cos I_{5\text{-}12}, \sin\alpha_2\sin I_{5\text{-}12}, \cos\alpha_2)$, where the angle $I_{5\text{-}12}$ is γ, 90°–γ, 90° + γ, 180°–γ, 180° + γ, 270°–γ, 270° + γ, and 360° – γ, respectively. Using Eq. (1), the interference intensity is calculated and shown in Fig. 3(a). The interference pattern has a large size of unit super-cell as indicated by the yellow square. Because the interfering angle α_1 is much larger than α_2, the interference pattern can approximately be understood as 1 – 4 beam interference with a small feature, modulated by 5 – 12 beam interference with a large feature. The interference among 1 – 4 beams can produce lattices with a lattice constant = $2\pi/(k\sin\alpha_1(\cos 45° - \cos 135°)) = \lambda/(\sqrt{2}\sin\alpha_1)$, where $\alpha_1 = \theta_1 f_1\sqrt{2}/f_2$. Thus the lattice constant Λ equals pixel-side-length/2 = 4 μm. The modulation of 1 – 4 beam interference in radial direction by the 5 – 12 beams can be characterized by a radius of a yellow circle in Fig. 3(a). The set of $(k_n - k_{n+2})$ among 5 – 12 beams forms a circle, for example, $(k_5 - k_7) = k\sin\alpha_2(2\sin(\gamma + 45°)\sin 45°, -2\cos(\gamma + 45°)\sin 45°, 0)$. The generated interference forms a modulation circle with a radius = $2\pi/(k\sin\alpha_2\sqrt{2}) = \lambda/(\sqrt{2}\sin\alpha_2) = 24$ pixel-side-length/4 = 48 μm = 12Λ, as shown by the red bar in Fig. 3(a). The solid yellow square in Fig. 3(a) has the unit super-cell size of 12Λ × 12Λ. There are 8 graded regions surrounding the central almost-uniform region as indicated by the yellow octagon in Fig. 3(a). When the number of side graded regions increases, these graded regions form super-cavity or the central almost-uniform region forms the cavity core in the hetero-structure photonic crystal [22].

Figure 3(b) shows the SEM image of fabricated GPSC in DPHPA mixture. The lattice constant Λ = 4 μm as measured in SEM. The red square indicates the unit super-cell of 12Λ × 12Λ. The 8 graded regions are connected by the dashed red octagon. The fabricated sample matches the simulated interference pattern. A square symmetry is

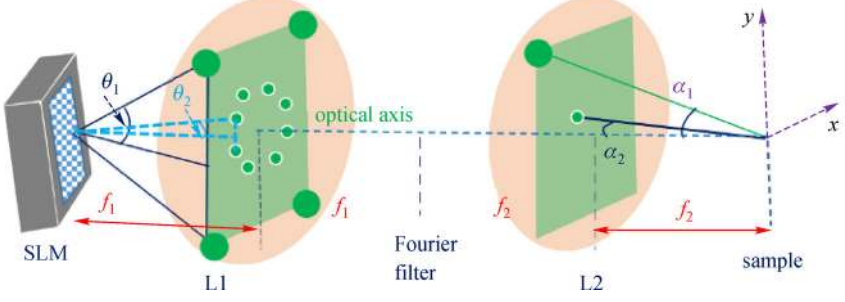

Fig. 2 Schematic of the optical setup for the holographic fabrication of octagon GPSC. The diffracted beams from the phase pattern displayed in SLM are filtered at the Fourier Plane and form interference patterns through 4*f* imaging system. θ_1 and θ_2 are the first order diffraction angles due to the periodic array of 2 pixels, 24 pixels, respectively. α_1 and α_2 (zenith angle) are the interfering angles of 1 –4 beams and 5 –12 beams in Fig. 1(b), respectively

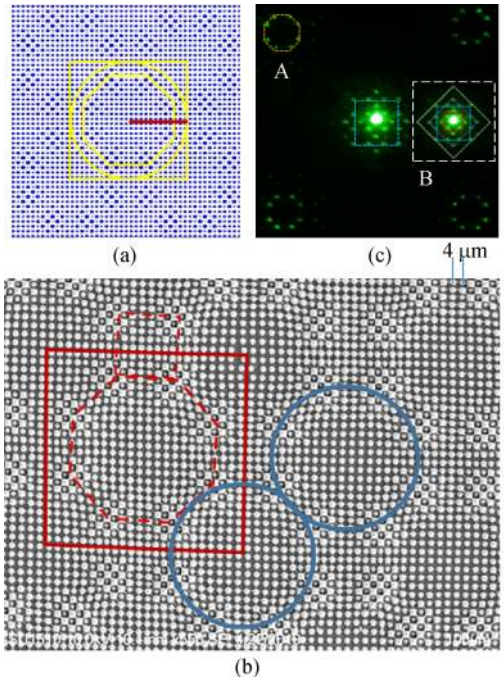

Fig. 3 (a) Simulated 12-beam interference pattern with 8 graded regions forming octagon and surrounding the central almost uniform region. The yellow square indicates the unit super-cell. (b) Scanning electron microscope (SEM) image of a fabricated sample where the 8 graded regions are connected by a dashed red octagon. The solid red square indicates the unit super-cell and both squares indicate a square symmetry. A lattice spacing parameter Λ = 4 μm. (c) Diffraction pattern of fabricated sample from 532 nm laser. An insert inside the dashed white square is a copy of pattern in the central region with 5 squares for eye guidance purpose. The yellow octagon is for eye guidance

obvious as seen from the unit super-cell and the dashed red square connecting 4 graded region at the unit super-cell boundary in Fig. 3(b). The square symmetry is also confirmed in the diffraction pattern of fabricated sample by 532 nm laser, as shown in Fig. 3(c). The insert inside the dashed white square is the copy of the diffraction pattern from the central region but with drawing of squares connecting the diffraction spots. We have used five squares in the insert to connect all spots, indicating the order of modulated lattices in fabricated sample. There are four diffraction regions at the each corner of the square in Fig. 3(c). One of them is indicated by the dashed yellow octagon. These spots contain the lattice information in the unit super-cell. The octagon diffraction in Fig. 3(c) spots correspond to 8 graded regions inside the unit super-cell in Fig. 3(b).

4 Discussion: prospect in applications in topological photonics

If the cathode of the organic light emitting is patterned with GPSC, the light extraction efficiency will be improved [23]. If silicon (dielectric constant = 12) is used in the GPSCs, the graded regions have several photonic band gaps while the central almost-uniform region has one photonic band gap [24]. There is no band gap in the boundary of the graded and uniform regions in certain frequency range due to the dislocation of photonic band gap in either sides. Figures 4(a) and 4(b) show simulated *E*-field distribution in the octagon GPSCs. These *E*-fields appear in the boundary. Usually the appearance of interface states are characteristic of topological photonics [25]. Further design at pixel levels in the phase pattern in SLM can be added into the square unit cell of the phase pattern for the generation of photonic structures with desired photonic band structures for the interface states [16,17].

The photonic band structure can also be engineered so that the *E*-fields are confined in the graded regions and coupled to form ring resonances as a side ring among the 8 graded region and as a link ring among the 4 graded regions as shown in Figs. 3(b), 4(b) and 4(c) for applications in topological photonics [26,27].

5 Conclusion

In this paper, we have fabricated octagon GPSCs through holographic lithography via a simple pixel-by-pixel phase

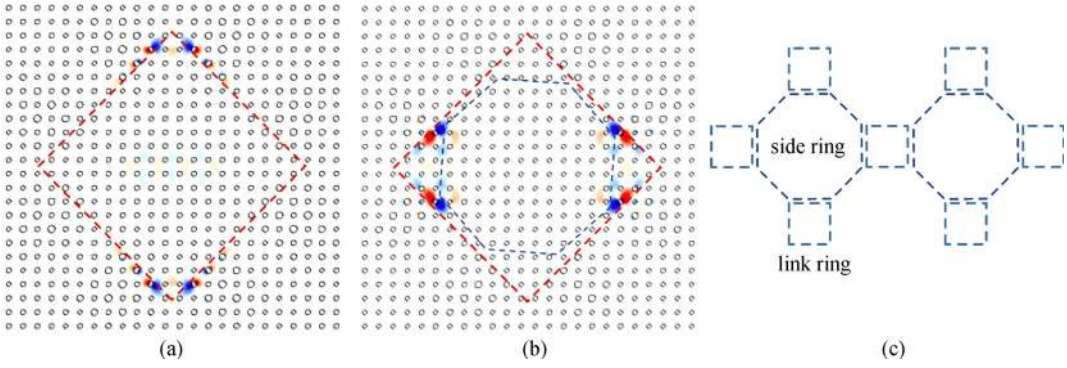

Fig. 4 (a) and (b) Simulated electric field distributions in the boundary of graded and uniform regions. (c) Possible side and link ring formation in octagon GPSCs

design in a square unit cell of phase pattern displayed in the digital SLM. The prospect of octagon GPSCs for topological photonics has been discussed.

Funding Information National Science Foundation (NSF) (Nos. 1661842 and 1661749).

References

1. Chanda D, Abolghasemi L E, Haque M, Ng M L, Herman P R. Multi-level diffractive optics for single laser exposure fabrication of telecom-band diamond-like 3-dimensional photonic crystals. Optics Express, 2008, 16(20): 15402–15414
2. Ohlinger K, Zhang H, Lin Y, Xu D, Chen K P. A tunable three layer phase mask for single laser exposure 3D photonic crystal generations: bandgap simulation and holographic fabrication. Optical Materials Express, 2011, 1(5): 1034–1039
3. Leach J, Wulff K, Sinclair G, Jordan P, Courtial J, Thomson L, Gibson G, Karunwi K, Cooper J, Laczik Z J, Padgett M. Interactive approach to optical tweezers control. Applied Optics, 2006, 45(5): 897–903
4. Xavier J, Dasgupta R, Ahlawat S, Joseph J, Gupta P K. Three dimensional optical twisters-driven helically-stacked multi-layered microrotors. Applied Physics Letters, 2012, 100(12): 121101
5. Zito G, Piccirillo B, Santamato E, Marino A, Tkachenko V, Abbate G. Two-dimensional photonic quasicrystals by single beam computer-generated holography. Optics Express, 2008, 16(8): 5164–5170
6. Jenness N J, Wulff K D, Johannes M S, Padgett M J, Cole D G, Clark R L. Three-dimensional parallel holographic micropatterning using a spatial light modulator. Optics Express, 2008, 16(20): 15942–15948
7. Arrizón V, de-la-Llave D S, Méndez G, Ruiz U. Efficient generation of periodic and quasi-periodic non-diffractive optical fields with phase holograms. Optics Express, 2011, 19(11): 10553–10562
8. Xavier J, Rose P, Terhalle B, Joseph J, Denz C. Three-dimensional optically induced reconfigurable photorefractive nonlinear photonic lattices. Optics Letters, 2009, 34(17): 2625–2627
9. Xavier J, Joseph J. Tunable complex photonic chiral lattices by reconfigurable optical phase engineering. Optics Letters, 2011, 36 (3): 403–405
10. Xavier J, Vyas S, Senthilkumaran P, Denz C, Joseph J. Sculptured 3D twister superlattices embedded with tunable vortex spirals. Optics Letters, 2011, 36(17): 3512–3514
11. Behera S, Joseph J. Single-step optical realization of bio-inspired dual-periodic motheye and gradient-index-array photonic structures. Optics Letters, 2016, 41(15): 3579–3582
12. Lutkenhaus J, George D, Moazzezi M, Philipose U, Lin Y. Digitally tunable holographic lithography using a spatial light modulator as a programmable phase mask. Optics Express, 2013, 21(22): 26227–26235
13. Kumar M, Joseph J. Optical generation of a spatially variant two-dimensional lattice structure by using a phase only spatial light modulator. Applied Physics Letters, 2014, 105(5): 051102
14. Rumpf R C, Pazos J. Synthesis of spatially variant lattices. Optics Express, 2012, 20(14): 15263–15274
15. Digaum J L, Pazos J J, Chiles J, D'Archangel J, Padilla G, Tatulian A, Rumpf R C, Fathpour S, Boreman G D, Kuebler S M. Tight control of light beams in photonic crystals with spatially-variant lattice orientation. Optics Express, 2014, 22(21): 25788–25804
16. Lutkenhaus J, George D, Lowell D, Arigong B, Zhang H, Lin Y. Registering functional defects into periodic holographic structures. Applied Optics, 2015, 54(23): 7007–7012
17. Lutkenhaus J, Lowell D, George D, Zhang H, Lin Y. Holographic fabrication of designed functional defect lines in photonic crystal lattice using a spatial light modulator. Micromachines, 2016, 7(4): 59
18. Lowell D, Lutkenhaus J, George D, Philipose U, Chen B, Lin Y. Simultaneous direct holographic fabrication of photonic cavity and graded photonic lattice with dual periodicity, dual basis, and dual symmetry. Optics Express, 2017, 25(13): 14444–14452
19. Lowell D, Hassan S, Sale O, Adewole M, Hurley N, Philipose U, Chen B, Lin Y. Holographic fabrication of graded photonic super-quasi-crystals with multiple-level gradients. Applied Optics, 2018, 57(22): 6598–6604
20. Lowell D, Hassan S, Adewole M, Philipose U, Chen B, Lin Y. Holographic fabrication of graded photonic super-crystals using an integrated spatial light modulator and reflective optical element laser projection system. Applied Optics, 2017, 56(36): 9888
21. Hassan S, Sale O, Lowell D, Hurley N, Lin Y. Holographic fabrication and optical property of graded photonic super-crystals with a rectangular unit super-cell. Photonics, 2018, 5(4): 34
22. Ge X, Minkov M, Fan S, Li X, Zhou W. Low index contrast heterostructure photonic crystal cavities with high quality factors and vertical radiation coupling. Applied Physics Letters, 2018, 112 (14): 141105
23. Hassan S, Lowell D, Lin Y. High light extraction efficiency into glass substrate in organic light-emitting diodes by patterning the cathode in graded superlattice with dual periodicity and dual basis. Journal of Applied Physics, 2017, 121(23): 233104
24. Hassan S, Alnasser K, Lowell D, Lin Y. Effects of photonic band structure and unit super-cell size in graded photonic super-crystal on broadband light absorption in silicon. Photonics, 2019, 6(2): 50
25. Lu L, Joannopoulos J D, Soljačić M. Topological photonics. Nature Photonics, 2014, 8(11): 821–829
26. Bandres M A, Wittek S, Harari G, Parto M, Ren J, Segev M, Christodoulides D N, Khajavikhan M. Topological insulator laser: experiments. Science, 2018, 359: 4005
27. Ao Y, Hu X, Li C, You Y, Gong Q. Topological properties of coupled resonator array based on accurate band structure. Physical Review Materials, 2018, 2(10): 105201

Safaa Hassan received his B.S. and M.S. degrees in Physics from Mustansiriyah University, Baghdad, Iraq, in 2002 and 2005 respectively. In 2005 – 2008, he worked as a researcher in the College of Science/Department of Physics and College of Engineering, Mustansiriyah University, Baghdad, Iraq. In 2008 – 2013, he was hired as a Lecturer in the Department

of Physics/College of Science, Mustansiriyah University. He is a Ph. D. candidate at University of North Texas. His current research interests include holographic fabrication of photonic crystals and graded photonic super-crystals, light extraction in organic light emitting diode (OLED) and gradient index photonic devices.

Usha Philipose received her B.S, M.S. and M.Phil. degrees in Physics from University of Bombay, India. She received her Ph.D. degree in Materials Science and Engineering from University of Toronto, Canada, in 2006. She later worked as a postdoctoral researcher at the Centre for Advanced Nanotechnology, University of Toronto, Canada. She joined the Department of Physics at the University of North Texas, Denton in 2008 as an Assistant Professor. She received tenure and was promoted to the rank of an Associate Professor in 2014. Her current research interests include studying electron, photon and phonon transport in 1D nanostructures, as well as increasing the complexity of these structures to study effect on certain functionalities such as its optoelectronic and energy conversion capabilities.

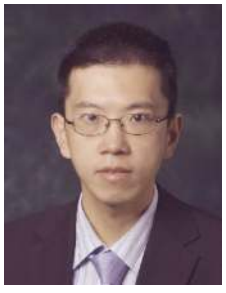

Hualiang Zhang is an Associate Professor at the Electrical and Computer Engineering Department, University of Massachusetts Lowell. He received his B.S. degree in Electrical Engineering from the University of Science and Technology of China in 2003. He received his Ph.D. degree in Electrical and Computer Engineering from the Hong Kong University of Science and Technology in 2007. From 2007 to 2009, he was a postdoctoral research associate in the Department of Electrical and Computer Engineering at the University of Arizona. From 2009 to Jan. 2016, he was a faculty member at the University of North Texas. His research interests include metamaterials, nano-photonics, optoelectronics, RF/microwave/millimeter-wave circuits and systems, antennas, and their applications. He is the co-author of over 200 journal and conference papers. Dr. Zhang is a senior member of IEEE.

Yuankun Lin received his B.S. and M.S. degrees in Physics from Nankai University, Tianjin, China, in 1991 and 1994, respectively. He received his Ph.D. degree in Physics from the University of British Columbia, Vancouver, Canada, in 2000. In 2000 – 2004, he worked as a postdoctoral research fellow in photonics group in the Department of Electrical and Computer Engineering, University of Toronto. Then he was hired as an Assistant Professor in 2004 and promoted to an Associate Professor in 2007 at University of Texas Pan American. In 2010, he was hired as an Associate Professor in the Department of Physics and Department of Electrical Engineering at the University of North Texas and promoted to Full Professor in 2015. His current research interests include holographic fabrication of photonic crystals and graded photonic super-crystals, light extraction in OLED, gradient index photonic devices and phase mask.